

## **Plio-Pleistocene decline of mesic forest underpins diversification in a clade of Australian *Panesthia* cockroaches**

Maxim W.D. Adams<sup>1\*</sup>, James A. Walker<sup>2</sup>, Harley A. Rose<sup>1</sup>, Braxton R. Jones<sup>1</sup>, Andreas Zwick<sup>3</sup>, Huiming Yang<sup>3</sup>, James Nicholls<sup>3</sup>, Diana Hartley<sup>3</sup>, Stephen Bent<sup>3</sup>, Nicholas Carlile<sup>4</sup>, Ian Hutton<sup>5</sup>, Simon Y.W. Ho<sup>1</sup>, Nathan Lo<sup>1\*</sup>

<sup>1</sup> School of Life and Environmental Sciences, University of Sydney, Sydney NSW 2006, Australia

<sup>2</sup> Australian Government Department of Agriculture Water and Environment, Canberra ACT 2601, Australia

<sup>3</sup> Australian National Insect Collection, CSIRO National Research Collections Australia, Canberra ACT 2601, Australia

<sup>4</sup> Ecosystems and Threatened Species, Department of Climate Change, Energy, the Environment and Water, Parramatta NSW 2124, Australia

<sup>5</sup> Lord Howe Island Museum, Lord Howe Island NSW 2898, Australia

### **\* Correspondence**

Maxim Adams, LEES Building F22, School of Life and Environmental Sciences, University of Sydney, Sydney NSW 2006, Australia

Email: [mada0372@uni.sydney.edu.au](mailto:mada0372@uni.sydney.edu.au)

Nathan Lo, LEES Building F22, School of Life and Environmental Sciences, University of Sydney, Sydney NSW 2006, Australia

Email: [nathan.lo@sydney.edu.au](mailto:nathan.lo@sydney.edu.au)

1    **Abstract**

2    The progressive aridification of the Australian continent, and coincident decline of mesic  
3    forest, has been a powerful driver of allopatric and environmental speciation in native  
4    species. The relictual mesic forests of the eastern seaboard now harbor a diverse group of  
5    endemic fauna, including the wood-feeding cockroaches of the genus *Panesthia*, which  
6    reached the continent via two separate invasions from Melanesia. The more recent of these  
7    colonization events gave rise to a group of five recognized species, occurring in mainland  
8    woodlands, sclerophylls and rainforests, as well as the forests and grasslands of the Lord  
9    Howe Island Group. Due to limited sampling in molecular studies and doubt regarding the  
10   standing taxonomy, there is little certainty about relationships among the species and poor  
11   understanding of the effects of ancient climatic changes upon their evolution. We undertook a  
12   comprehensive phylogenetic analysis of the clade, using complete mitogenomes and nuclear  
13   ribosomal markers from nearly all known morphospecies and populations. Our time-  
14   calibrated phylogenetic analyses reveal six unrecognized, highly divergent lineages, and  
15   suggest that these have arisen primarily through vicariance as rainforests fragmented during  
16   Plio-Pleistocene glacial cycles (2–5 million years ago). Ancestral niche reconstructions also  
17   evidence a tropical rainforest origin for the group, followed by at least three niche transitions  
18   into drier forest, including one associated with the singular colonization of the Lord Howe  
19   Island Group. Finally, we find evidence of frequent, parallel wing reduction, in potential  
20   association with the contraction of forest habitats into small refugia. Our results reiterate the  
21   far-reaching role of ancient aridification in driving speciation, niche expansion and  
22   morphological evolution in Australian fauna.

23

24    **Keywords:** systematics, biogeography, Australia, mesic biome, insects, *Panesthia*

## 25 1. Introduction

26 The mesic forests of eastern Australia are among the most biodiverse habitats in the  
27 world (Ebach, 2017; Williams et al., 2011b). Occurring in a peri-coastal distribution from  
28 Queensland to Victoria, these forests are the fragmented relics of the Gondwanan rainforests  
29 that once spanned the entire continent (Hill, 1994; White, 1986, 1994). This fragmentation,  
30 caused by the gradual aridification of the Miocene and the dramatic arid cycles of the Plio-  
31 Pleistocene, saw rainforests progressively replaced by drier sclerophyll and woodland  
32 elements, with transformative effects upon the mesic biota (Bryant and Krosch, 2016; Byrne  
33 et al., 2011; Harvey et al., 2017). Untangling the complex dynamics of vicariance, adaptation  
34 and niche transition remains a central goal in Australian biogeography.

35 A group of consequent interest are the saproxylic (dead wood-feeding) cockroaches of  
36 the genus *Panesthia*. Originating in Asia, the *Panesthia* invaded Australia in two independent  
37 waves in the middle and late Miocene, following the collision of the Sahul and Sundaland  
38 tectonic plates (Beasley et al., 2021b; Lo et al., 2016; Maekawa et al., 2003). The latter  
39 of these colonizations has attained a broad geographic range spanning mesic, sclerophyll and  
40 woodland forests across the Australian eastern seaboard, as well as the Lord Howe Island  
41 Group (LHIG), a volcanic archipelago ~600 km east of New South Wales (Beccaloni, 2014;  
42 Roth, 1977). Intriguingly, the insects themselves are highly sedentary and typically reside  
43 long-term within decaying logs. Many lineages have also undergone degrees of secondary  
44 wing reduction, rendering them completely flightless; while full-winged individuals manually  
45 remove their wings soon after the final molt, thereby losing flight capacity (Bell et al., 2007b;  
46 O'Neill et al., 1987). Their low vagility and habitat specificity position the group (hereafter  
47 “*Panesthia*”) as sensitive biogeographic indicators, and raise the question of how they were  
48 impacted by the fragmentation of mesic forest.

49 The clade comprises an ‘archipelagic’ array of isolated mesic lineages; as well as less  
50 wet-adapted species that have broader, contiguous distributions through the surrounding  
51 matrix of drier sclerophyll or open woodlands. The origins of the mesic populations remain  
52 contentious, with two broad models advanced across the literature. Based on the present  
53 habitats of Melanesian relatives, it has been suggested that the ancestral *Panesthia* were  
54 rainforest obligates (Maekawa et al., 2003), which presumably diversified through vicariance  
55 as mesic environments fragmented. This explanation would be consistent with many  
56 paradigmatic examples of allopatric speciation across the mesic biome (e.g. Bell et al., 2007a;  
57 Moreau et al., 2015; Oberski et al., 2018; Rix and Harvey, 2012). However, the distribution  
58 of mesic *Panesthia*, spanning the entire eastern seaboard, is unusually broad for a dispersal-  
59 limited invertebrate (reviewed by Bryant and Krosch, 2016), and their ancestral habitat  
60 remains poorly characterized. An alternative explanation is that the ancestors of the extant  
61 species had already come to inhabit dry sclerophyll or woodland, and subsequently colonized  
62 individual rainforest refugia as they dispersed (Beasley□Hall et al., 2021b). Transitions from  
63 dry, even arid, habitat to rainforest have been reported in a wide range of species (Byrne et  
64 al., 2018), including sedentary invertebrates (e.g., Rix et al., 2021). Interestingly, the most  
65 widespread taxon within the group, *Panesthia cibrata*, is known from both wet and dry  
66 sclerophyll, and shows a close morphological affinity to multiple, geographically separated  
67 rainforest lineages.

68 The most divergent habitat niche is now observed in *P. lata*, which is endemic to the  
69 LHIG. Estimated to have colonized the archipelago 2–6 million years ago (Lo et al., 2016),  
70 the species occupies rainforest on Lord Howe Island itself, and more exposed grasslands on  
71 several of the surrounding islets. The cockroaches are also unique in constructing shallow  
72 burrows under stones or leaf litter, rather than inhabiting logs (Rose, 2003). It has been  
73 suggested that the offshore islet populations expanded their niche *in situ* in response to the

74 exposed conditions of the archipelago (Beasley□Hall et al., 2021b). However, without a clear  
75 understanding of the ancestral habitat of mainland congeners, and of the species itself, the  
76 evolution of environmental tolerances of *P. lata* remains opaque.

77 To date, biogeographic understanding has been limited by systematic irresolution. The  
78 monophyly of the *Panesthia* is well supported, yet estimates of the relationships within the  
79 group have been highly unstable between studies (Beasley□Hall et al., 2021b; Legendre et  
80 al., 2017; Legendre et al., 2015; Lo et al., 2016). While five species are presently recognized,  
81 there is mounting evidence of discordance between genetic results and the morphology-based  
82 taxonomy, suggesting cryptic speciation and phenotypic parallelism (Beasley□Hall et al.,  
83 2021b; Djernæs et al., 2020; Lo et al., 2016). Previous investigations have included only few  
84 representatives of the clade and have lacked the resolution to confidently delimit species or  
85 interrogate geographic patterns of diversity.

86 Here we undertake the first comprehensive phylogenetic investigation of the  
87 *Panesthia*, including novel populations never previously examined in taxonomic or genetic  
88 studies. In clarifying their systematics and evolutionary history, we explore three  
89 fundamental questions: 1) Did the contemporary distribution of mesic lineages arise through  
90 vicariance, or were these habitats separately colonized by dry-forest ancestors?; 2) Were the  
91 ancestors of *P. lata* pre-adapted to the drier conditions of the LHIG, or did the species expand  
92 its niche following island colonization?; and 3) Do flightless morphs share a common  
93 ancestry, or has wing reduction occurred in parallel? The results of our study highlight the  
94 complex evolutionary dynamics associated with Australia's mesic biome.

95

96 **2. Methods**

97 *2.1. Sampling and DNA sequence data*

98 Samples of mainland taxa were collected between 1998 and 2023 from across New  
99 South Wales and Queensland, Australia. Specimens were stored in 70–100% ethanol or in  
100 pinned collection prior to DNA extraction, and are presently held in the private collections of  
101 H.A. Rose and J.A. Walker. Due to the scarcity of *P. lata* in collection, we retrieved  
102 specimens from the LHIG in July and August of 2022, from Blackburn Island, Roach Island  
103 and a newly discovered relict population on Lord Howe Island (Adams et al., in prep.). In  
104 supplement, we subsampled tissue from historical specimens of *P. lata* collected on Lord  
105 Howe Island and Ball's Pyramid between 1869 and 1973, sourced from the Australian  
106 Museum, Sydney and the Macleay Museum, Sydney. A full list of material with GenBank  
107 accession numbers is provided in Supplementary Table S1.

108 DNA was extracted from leg muscle tissue to avoid contamination from  
109 *Blattabacterium* bacterial endosymbionts, which occur in abdominal fat bodies (Kinjo et al.,  
110 2015). DNA sequencing was outsourced to the Australian National Insect Collection,  
111 Canberra, utilizing an approach suitable for highly fragmented historical DNA (see Jin et al.,  
112 2020; Zwick and Zwick, 2023 for methods). In summary, genomic DNA was extracted using  
113 proteinase K digestion and a silica filter-based approach in a 384-well format. Up to 5 ng of  
114 extracted DNA were used to build ligation-based whole-genome shotgun DNA sequencing  
115 libraries, utilizing an acoustic liquid handler (Echo 525; Beckman Coulter, California, USA)  
116 to miniaturize reaction volumes for increased reaction efficiency. DNA libraries of different  
117 samples were pooled equimolar and sequenced at the Australian National University's  
118 Biomolecular Resource Facility on an Illumina NovaSeq 6000 platform, using an S1 flow cell  
119 and a 300-cycle sequencing kit. The output of 1.65 billion 150 bp paired-end reads were  
120 demultiplexed to yield a median of 27,321 reads per sample. Output data included reads from

121 most or all of the mitochondrial genome (hereafter “mitogenome”), as well as the nuclear  
122 ribosomal operon (which encodes 18S, 5.8S and 28S ribosomal RNA, alongside the internal  
123 transcribed spacers *ITS1* and *ITS2*).

124 We assembled raw reads into contigs using SPAdes v.3.12.0 (Bankevich et al., 2012)  
125 with default settings and sampling  $k$  values of 33, 55, 77, 91, and 121. To generate  
126 mitogenomes, contigs produced in SPAdes were imported into Geneious Prime v.2022.1.1  
127 (<https://www.geneious.com>) and assembled to a reference sequence using the Map to  
128 Reference tool with default settings and medium sensitivity. Where available, we extracted  
129 the single contig comprising the near-complete mitogenome (*ca.* 15,000 bp). Otherwise, we  
130 extracted the consensus sequence of multiple contigs, selecting the bases with the highest  
131 representation. Reference sequences were chosen to represent the closest known sister taxon  
132 to each sample, based on the phylogenetic framework of Beasley-Hall et al. (2021b); these  
133 were sourced from GenBank or from mitogenomes generated presently.

134 We annotated mitogenomes using the MITOS web server (Bernt et al., 2013) under  
135 default settings for invertebrate mitochondrial DNA. Duplicated annotations and split genes  
136 were corrected in Geneious, and we checked for errors against published references for  
137 *Panesthia parva*, *Panesthia sloanei* and *Panesthia angustipennis* (Beasley-Hall et al.,  
138 2021b). We then aligned the sequences for each gene individually using the MUSCLE  
139 algorithm (Edgar, 2004) within Geneious. The control region was omitted from our analyses,  
140 as it includes repetitive DNA regions that are not reliably assembled from short reads  
141 (Bourguignon et al., 2018). Nuclear markers were generated via the same steps, initially  
142 using a nuclear ribosomal operon reference sequence for *Panesthia angustipennis*  
143 (comprising, in order, *18S*, *ITS1*, *5.8S*, *ITS2* and *28S*; Che et al., 2022). The final  
144 mitochondrial and nuclear alignments represented a total of 14,707 bp and 5,596 bp,  
145 respectively, and were analysed separately to account for potential genealogical discordance.

146 One novel morphospecies, known from Koombooloomba State Forest, Queensland,  
147 was discovered after the main round of sequencing. We used polymerase chain reaction  
148 (PCR) amplification to generate a 604 bp fragment of mitochondrial *COI* and a 352 bp  
149 fragment of mitochondrial *16S* from a single specimen (see Supplementary Table S2 for  
150 primers and PCR protocols). Econotaq<sup>TM</sup> master mix (New England Biolabs, Massachusetts,  
151 USA) was used as the source of free nucleotides and reaction buffers. PCR products were  
152 cleaned using Exosap-IT (Thermo Fisher Scientific, Massachusetts, USA) and sent to  
153 Macrogen (Seoul, Gyeonggi, South Korea) for Sanger sequencing.

154 In total, 137 ingroup taxa were sequenced successfully. We combined these sequences  
155 with a complete mitogenome of the ingroup taxon *Panesthia parva*, and six outgroup  
156 representatives of the Australian and Melanesian Panesthiinae, which were retrieved from  
157 GenBank (Supplementary Table S1). Each gene alignment was manually checked for reading  
158 frames and premature stop codons in Seqtron v.1.0.1 (Fourment and Holmes, 2016), and  
159 ambiguously aligned regions were removed. We then tested for substitutional saturation using  
160 Xia's method in DAMBE7 (Xia, 2018), and in its absence retained all codon positions for  
161 analysis.

162

## 163 2.2. Phylogenetic analysis

164 For the mitochondrial data set, we opted for a biologically relevant partitioning  
165 scheme consisting of first, second and third codon positions of protein-coding genes, rRNAs  
166 and tRNAs, in accordance with previous phylogenomic studies of the Blattodea  
167 (Beasley□Hall et al., 2021b; Bourguignon et al., 2014; Bourguignon et al., 2018; Cameron et  
168 al., 2012). However, we modified the scheme by implementing a separate partition for *COI*,  
169 to enable calibration of the molecular clock (for a total of six partitions). We used the  
170 ModelFinder function (Kalyaanamoorthy et al., 2017) to infer the best-fitting substitution

171 model for each partition, based on Bayesian information criterion scores (Supplementary  
172 Table S3). For the nuclear data set, we co-estimated the optimal scheme and substitution  
173 model using ModelFinder (2 partitions: *I8S+5.8S+28S*, *ITS1+ITS2*; Supplementary Table  
174 S3). This scheme was also modified for molecular dating by implementing a separate  
175 partition for *28S* (for a total of three partitions). Preliminary analyses showed that the  
176 segregation of *CO1* and *28S* did not affect the inferred tree topologies.

177 Maximum-likelihood (ML) phylogenetic analyses were performed in IQTREE v.2.2.2  
178 (Minh et al., 2020). Node support was estimated using 10,000 ultrafast bootstrap replicates  
179 (UFBoot; Hoang et al., 2018) and the SH-like approximate likelihood-ratio test (SH-aLRT)  
180 with 1,000 iterations. Following recommendations of the package, we considered UFBoot >  
181 0.95 and SH-aLRT > 0.8 to indicate strong support.

182 We undertook two additional analyses to investigate the discordance of the  
183 mitogenomic and nuclear topologies (see Results). First, we tested whether the signal from  
184 the nuclear data set was significantly inconsistent with the mitogenomic results. Using  
185 IQTREE, we analysed the nuclear markers under topology constraints following the species-  
186 level branching order of the mitogenomic ML topology, and statistically compared its  
187 adequacy relative to the unconstrained nuclear tree using six different metrics  
188 (Supplementary Table S4). Second, to assess the relative information content of the two data  
189 sets, we estimated ML and Bayesian trees using a concatenated alignment comprising all  
190 mitochondrial and nuclear loci. Partitions and substitution models were as described  
191 previously.

192

### 193 2.3. Molecular dating

194 Phylogenetic trees and evolutionary timescales were jointly estimated using Bayesian  
195 inference in BEAST v.10.4 (Suchard et al., 2018). We modeled among-lineage rate variation

196 using an uncorrelated lognormal relaxed clock (Drummond et al., 2006) and specified a birth-  
197 death tree prior, which is most appropriate for the combination of interspecific and  
198 intraspecific sampling in the data set (Ritchie et al., 2016). Each partition was assigned a  
199 separate GTR+I+G substitution model, representing the closest model to those estimated in  
200 ModelFinder. We ran two independent chains, drawing samples every  $10^3$  steps until  
201 convergence was observed in Tracer v.1.7.2 (Rambaut et al., 2018) and the effective sample  
202 size for each parameter reached  $\geq 200$  ( $1.5 \times 10^8$  steps for the mitogenomic data set,  $1 \times 10^8$   
203 steps for the nuclear data set). The maximum-clade-credibility tree was generated in  
204 TreeAnnotator with a 10% burn-in.

205 There are no known fossil calibrations proximal to the Mio-Pliocene divergences  
206 inferred for the *Panesthia* (Beasley□Hall et al., 2021b; Lo et al., 2016). We consequently  
207 utilized two different techniques to estimate the evolutionary timescale. First, we followed  
208 Beasley□Hall et al. (2021a) to specify an informative prior distribution for the substitution  
209 rate, based on the late Miocene diversification of Mediterranean *Dolichopoda* crickets  
210 (Allegrucci et al., 2011). The genus is ecologically and biologically similar to the *Panesthia*,  
211 comprising nonvagile, subterranean species of comparable body size (Allegrucci et al., 2021).  
212 In addition, the diversification of *Dolichopoda*, initiating *ca.* 7 Ma, is temporally proximal to  
213 the Mio-Pliocene radiation of the *Panesthia* estimated by Beasley□Hall et al. (2021b). For  
214 the mitogenomic analysis, we specified a substitution rate prior for *COI* ( $1.6 \times 10^{-2} \pm 1.1 \times 10^{-4}$   
215 substitutions/site/Myr), due to its conserved substitution rate across insect orders (Gaunt and  
216 Miles, 2002; Papadopoulou et al., 2010). For the nuclear analysis, the only available rate  
217 estimate was for *28S* ( $6.4 \times 10^{-4} \pm 4 \times 10^{-6}$  substitutions/site/Myr). These were applied as  
218 normal priors with uncertainty corresponding to the standard deviation, and the rates of  
219 remaining partitions were estimated during analysis.

220 For our second approach, we applied two secondary calibrations to the backbone  
221 nodes of the tree, based on the evolutionary timescale inferred by Beasley □ Hall et al.  
222 (2021b). Using the mitogenomic data set, we specified normal priors for the age of the root  
223 (29.18 ± 4.06 Ma) and for the node uniting *Panesthia* with the *P. angustipennis* complex  
224 (25.02 ± 5.42 Ma). Because the date estimates in Beasley □ Hall et al. (2021b) were inferred  
225 using ancient fossil calibrations, which tend to artifactually deepen shallow nodes (Hipsley  
226 and Müller, 2014; Ho et al., 2011), we consider the second approach to represent a  
227 conservative upper bound and primarily focus on results from the *Dolichopoda* rate of  
228 evolution.

229

230 *2.4. Species delimitation*

231 To investigate the presence of unrecognized species diversity, we followed a two-step  
232 process to delimit highly divergent, monophyletic clades (hereafter “operational taxonomic  
233 units”, or OTUs; see Supplementary Material for full methods). First, we generated OTU  
234 hypotheses *de novo* from the mitogenomic data set using the Generalized Mixed Yule  
235 Coalescent (GMYC; Zhang et al., 2013) and the distance-based Assemble Species by  
236 Automatic Partitioning (ASAP; Puillandre et al., 2021). Then, in accordance with best  
237 practice outlined by Carstens et al. (2013), we validated the output delimitations in Bayesian  
238 Phylogenetics and Phylogeography v.4.1.4 (BPP; Yang, 2015), using both the mitogenomic  
239 and nuclear data sets.

240

241 *2.5. Historical biogeography and niche evolution*

242 We reconstructed ancestral geographic ranges and habitat niches using the ultrametric  
243 phylogeny inferred in BEAST, with the input tree pruned to include a single representative of

244 each OTU. Due to the instability of the nuclear topology across analyses (see Results),  
245 reconstructions were only performed with the mitochondrial data set.

246 We explored changes in geographic range with the R package BioGeoBEARS  
247 (Matzke, 2013). Taxa were divided among five biogeographic zones: North Queensland,  
248 Central Queensland, Mid-Eastern Australia, South-Eastern Australia, and the LHIG. These  
249 correspond to zoogeographical subregions outlined by Ebach et al. (2013), which reflect well-  
250 documented partitions in the distributions of eastern seaboard fauna. Colonization of the  
251 LHIG was assumed to be unidirectional, while all other transitions were coded as  
252 equiprobable and time-constant. Based on contemporary ranges, the maximum number of  
253 areas was set as two.

254 We compared three widely applied biogeographic models, each with unique  
255 assumptions about the cladogenetic and anagenetic processes underpinning speciation. These  
256 were Dispersal-Extinction-Cladogenesis (DEC), Dispersal-Vicariance analysis (DIVA-like)  
257 and Bayesian Analysis of Biogeography (BayArea-like). Models were run under default  
258 parameters and compared using the corrected Akaike information criterion (AICc). We opted  
259 not to include the jump dispersal parameter (+J) due to ongoing debate regarding its  
260 statistical validity (Matzke, 2022; Ree and Sanmartín, 2018).

261 We also explored the timing of transitions between wet, dry, and open forest using  
262 ancestral niche reconstruction in the R package *Nichevol* v.1.19 (Owens et al., 2020). Species  
263 were split across three major habitat categories (following Braby et al., 2020; Mitchell et al.,  
264 2014): closed forest (rainforest, wet sclerophyll or vine thicket; canopy cover > 80%,  
265 precipitation:evaporation > 0.4), open forest (dry sclerophyll and scrub; canopy cover 50–  
266 80%) and woodland (canopy cover < 50%). We then modeled the change in habitat along the  
267 phylogeny using a maximum-likelihood framework. To avoid overestimating niche lability  
268 (Barve et al., 2011; Owens et al., 2020), *Nichevol* allows the presence of a taxon in a niche to

269 be coded as “uncertain”. We considered a niche to be uncertain unless the species was  
270 confirmed to be absent from the niche in an area adjacent to its known habitat. Ecological  
271 data were compiled from the personal observations of H. A. Rose and J. A. Walker and  
272 validated against the Cockroach Species File Online database (Beccaloni, 2014).

273

274 *2.6. Evolution of flight loss*

275 Lastly, we modeled the evolution of wing morphology using ancestral state  
276 reconstructions (ASRs). We classified OTUs as fully winged (macropterous), partially  
277 winged (brachypterous) or vestigially winged (micropterous) (see Figure 4 for representative  
278 images). Present-day characters were mapped onto our mitogenomic species tree, and ASRs  
279 were performed in the R package *phytools* v.2.1.1 (Revell, 2012). We reconstructed changes  
280 along the topology using a continuous-time Markov chain model, and estimated the most  
281 likely state at each node. The *Panesthia* are understood to have originated from macropterous  
282 ancestors (Lo et al., 2016), thus we included the closest known outgroup species *P.*  
283 *angustipennis angustipennis*, and fixed the root of the tree to be macropterous. We undertook  
284 two reconstructions, the first with a unidirectional rate matrix permitting only evolution away  
285 from the ancestral state (since wing re-evolution is considered highly unlikely; Trueman et  
286 al., 2004). Our second reconstruction permitted free transitions between all character states  
287 (by specifying a bidirectional “all rates different” model). As one OTU was found to be  
288 highly polymorphic, we undertook separate analyses reconstructing wing evolution within the  
289 OTU, using a single representative from each sampling locality.

290 **3. Results**

291 *3.1. Phylogenetic relationships and species delimitation*

292 Our analyses uniformly support the monophyly of the *Panesthia*. Maximum-  
293 likelihood and Bayesian analyses of the mitogenomic data set produced near-identical  
294 estimates of the phylogeny, differing only in the placements of some terminal branches  
295 (Figure 1). Genetic relationships within and between major lineages were generally clustered  
296 by geographic locality, with the northern Queensland samples (Clades A+B + *P. sp.*  
297 Koombooloomba) forming successive sister groups to a clade comprising samples from  
298 central and southern Queensland, New South Wales, and the LHIG (Clade C).

299 The three species delimitation methods applied to this data set yielded similar  
300 estimates of OTUs: 10 from GMYC, 12 from ASAP and 11 from BPP (Figure 1). Since the  
301 BPP analysis incorporated both mitochondrial and nuclear markers, and produced  
302 delimitations that best reflect accepted species boundaries, we consider the 11-OTU scheme  
303 to be the most robust and refer to this in subsequent sections.

304 Four of the OTUs correspond to novel localities previously unsampled in taxonomic  
305 or genetic studies: *P. sp.* Cape Upstart, *P. sp.* Airlie Beach, *P. sp.* Mt. Windsor and *P. sp.*  
306 Koombooloomba. Further, *P. cibrata* was found to comprise three divergent clades, which  
307 we presently refer to as *P. cibrata* North, *P. cibrata* Central and *P. cibrata* South. The  
308 monophyly of each OTU was well supported (excluding *P. sp.* Koombooloomba and *P. sp.*  
309 Mt. Windsor, each of which was represented by a single sample). The phylogenetic positions  
310 of all OTUs were also resolved with uniformly high support (PP, UFBoot, SH-aLRT > 0.95),  
311 excepting the crown node of Clade B (PP = 0.97, UFBoot = 0.9, SH-aLRT = 69.5) and the  
312 node uniting *P. sp.* Koombooloomba with its sister group (PP = 0.91, UFBoot = 0.97, SH-  
313 aLRT = 84.3; but note that only two markers were sequenced for this sample).

314 The mitochondrial OTUs were consistently recovered as monophyletic in our analyses  
315 of the nuclear ribosomal loci, with the exception of *P. cibrata* Central and *P. cibrata* South,  
316 which were paraphyletic in the ML and Bayesian trees, respectively (Figure 2,  
317 Supplementary Figure S1; note that *P. sp.* Koombooloomba was absent from the nuclear data  
318 set). However, the branching order of the OTUs and the populations within OTUs were  
319 somewhat discordant with the mitochondrial results, and differed between ML and Bayesian  
320 analyses (in both cases with relatively low node support; Figure 2, Supplementary Figure S1).  
321 The most significant conflict was the position of *P. lata*, which was placed substantially  
322 deeper in the phylogeny, either on its own branch in ML analysis (UFBoot = 46, SH-aLRT =  
323 60.7) or as sister to *P. sp.* Airlie Beach in Bayesian analysis (PP = 0.95).

324 The constrained nuclear tree, which followed the mitogenomic branching order, was  
325 strongly rejected by all six metrics in IQTREE in favor of the unconstrained tree  
326 (Supplementary Table S4), indicating that the phylogenetic signal from the nuclear data is  
327 significantly incongruent with the mitogenomic topology. However, when we estimated an  
328 ML tree from a concatenated alignment comprising all available loci, the species-level  
329 topology was almost identical to the mitogenomic tree, differing solely in the placement of *P.*  
330 *lata* as sister to *P. cibrata* Central + South (UFBoot = 98, SH-aLRT = 99.8; Supplementary  
331 Figure S2).

332

### 333 3.2. Molecular dating

334 Based on *CO1* rate calibration of the mitogenomic data set, the stem age of the  
335 *Panesthia* was placed at *ca.* 7.62 Ma (95% credible interval [CI] 5.79–9.53 Ma), with a  
336 crown age of *ca.* 5.30 Ma (95% CI 4.06–6.66 Ma). The stem ages of all eleven OTUs were  
337 dated to the Pliocene or early Pleistocene (*ca.* 1.8–5 Ma), with intraspecific divergences

338 occurring in the middle to late Pleistocene (< 1.5 Ma, excluding the Ball's Pyramid lineage of  
339 *P. lata*, which diverged from conspecifics *ca.* 1.51 Ma, 95% CI 1.08–1.96 Ma).

340 The evolutionary timescale recovered from nuclear loci yielded a curiously deep stem  
341 age, albeit with a broad 95% CI (14.61 Ma, 95% CI 5.16–24.82 Ma). The remaining nodes  
342 had younger and less precise age estimates than in the mitogenomic analysis (Supplementary  
343 Figure S1). The crown age of the *Panesthia* was estimated as *ca.* 4.84 Ma (95% CI 2.47–7.84  
344 Ma), while all species-level cladogenesis was estimated to have occurred in the late Pliocene  
345 and early–middle Pleistocene (*ca.* 0.5–3 Ma).

346 As anticipated, secondary calibration using node ages from Beasley□Hall et al.  
347 (2021b) produced a substantially deeper estimated timescale, with a stem age of 22.41 Ma  
348 (95% CI 15.46–28.89 Ma; Supplementary Figure S3). All interspecific divergences were  
349 estimated to have occurred in the middle to late Miocene (*ca.* 5.3–15.3 Ma), followed by  
350 intraspecific diversification throughout the Pliocene and Pleistocene (< 5.0 Ma).

351

### 352 3.3. *Historical biogeography*

353 In BioGeoBEARS analysis, the best-fitting model was DIVA-like (AICc = 49.64),  
354 compared with DEC (AICc = 50.78) and BayArea-like (AICc = 57.65). The ancestral state  
355 was well resolved (most probable state > 50%) for nearly all internal nodes, excluding only  
356 the clade comprising *P. lata* + *P. cibrata* South. Under this scenario, the most recent  
357 common ancestor (MRCA) of the *Panesthia* occurred in North Queensland (Figure 3). All  
358 ancestral and contemporary ranges in Clades A+B were placed in Central Queensland, while  
359 the crown node of Clade C was estimated to occur in Central Queensland alone, suggesting a  
360 southward range expansion. Presently, all mainland OTUs except *P. cibrata* South occur in  
361 Central or North Queensland, while the latter is found in Mid-eastern Australia and South-  
362 eastern Australia. The ancestral range of *P. lata*, which is presently endemic to the LHIG,

363 could not be confidently resolved between Central Queensland, Mid-eastern Australia, or  
364 South-eastern Australia.

365 Ancestral niche reconstruction in *Nichevol* suggested that the MRCA of the *Panesthia*  
366 inhabited exclusively closed forest (Figure 3). This niche was retained in the ancestors of all  
367 lineages in Clades A + B; however, we inferred a niche expansion into open forest within  
368 Clade C, occurring in the ancestor of *P. matthewsi* + *P. cibrata* Central + *P. lata* + *P.*  
369 *cibrata* South. In addition, two contemporary OTUs were found to have independently  
370 expanded or shifted their niche into woodland: *P. parva*, which inhabits woodlands only; and  
371 *P. lata*, which inhabits mesic closed forest, open forest, woodland and xeric grasslands (not  
372 labeled). No mesic lineages were found to have evolved from dry forest or woodland  
373 ancestors.

374

375 *3.4. Wing morphology*

376 Ancestral state reconstructions consistently found that wing reduction has occurred  
377 multiple times within the *Panesthia*. When wing re-evolution was prohibited, wing reduction  
378 was inferred to have occurred six times in total, including twice within *P. cibrata* Central  
379 (Figure 4). Five OTUs were exclusively micropterous, arising from four independent wing  
380 reductions: *P. lata*, *P. matthewsi*, *P. cibrata* North, and *P. sp.* Cape Upstart + *P. sp.* Brandy  
381 Creek (Figure 4a). In contrast, *P. cibrata* Central was found to be wing polymorphic. When  
382 wing evolution was modeled within the species, we inferred two populations to have  
383 independently become brachypterous (Murgon and Kroombit Tops) and a single population  
384 to have become micropterous (Gayndah), having evolved from a shared, brachypterous  
385 ancestor with the Kroombit Tops population (Figure 4b).

386 The scenario varied slightly when wing re-evolution was permitted, with an estimate  
387 of eight independent wing reductions (Supplementary Figure S4). All flightless lineages were  
388 inferred to have independently arisen from macropterous ancestors, including *P. sp.* Cape  
389 Upstart and *P. sp.* Airlie Beach, and the Gayndah and Kroombit Tops populations of *P.*  
390 *cribrata* Central.

391 **4. Discussion**

392

393 *4.1. Phylogenetic relationships*

394 This study substantially clarifies the evolution and systematics of the *Panesthia*.

395 Previously thought to comprise five species, our results reveal unrecognized diversity in

396 rainforest isolates across Queensland, and we provisionally identify eleven divergent

397 lineages. With the notable exception of *P. cibrata*, there was strong support for the

398 monophyly of established species in both nuclear and mitochondrial analyses. In contrast,

399 geographic sampling was sufficient to discern three divergent mitochondrial clades within *P.*

400 *cibrata*, which were polyphyletic with respect to *P. lata* and *P. matthewsi*. This potentially

401 explains the inconsistent relationships between these species across previous studies

402 (Beasley□Hall et al., 2021b; Lo et al., 2016), and echoes suggestions that *P. cibrata*

403 represents a species complex (Beasley□Hall et al., 2021b; Roth, 1977). However, we are

404 currently unable to discern morphological boundaries between the three *cibrata* lineages,

405 and note that the non-monophyly *P. cibrata* South and Central in nuclear analyses may

406 indicate ongoing gene flow at the boundary of their ranges. Taxonomic study is underway to

407 determine whether and how to partition the putative complex, as well as to formally describe

408 the novel OTUs identified by our study.

409 Mitogenomic analyses supported a southward grade of diversification, with all north

410 Queensland samples forming successive sister lineages to those present in south-east

411 Queensland and New South Wales. This is consistent with the understanding that the

412 *Panesthia* dispersed southwards across Australia following their arrival from Melanesia

413 (Maekawa et al., 2003). A similar overall pattern was found by Lo et al. (2016) and Beasley-

414 Hall et al. (2021b), using primarily mitochondrial markers with lower taxon sampling.

415 Although the nuclear topologies also supported a north–south geographical gradient, the trees

416 were less strictly geographically clustered, and estimated an early divergence of *P. lata*. This  
417 aligns with the results of Legendre et al. (2015, 2017), where *P. lata* was inferred to be sister  
418 to a clade uniting *P. cibrata* and *P. ancaudelliooides*, based on analysis of concatenated  
419 mitochondrial and nuclear genes.

420 Mito-nuclear discordance is not unusual in data sets spanning the boundary between  
421 species- and population-level processes, and could indicate incomplete lineage sorting,  
422 selection or introgression. Nuclear introgression would be consistent with the male-biased  
423 dispersal observed in *Panesthia* species (O'Neill et al., 1987). However, given the slower  
424 evolution and low node support of the nuclear phylogenies, it is likely that much of the  
425 discordance is due to low phylogenetic information content (Zink and Barrowclough, 2008).  
426 This interpretation is broadly supported by our analyses of the concatenated data set, which  
427 produced a topology almost identical to that inferred from mitogenomes. Therefore, we focus  
428 our discussions on the mitogenomic results, noting well-supported discrepancies where  
429 relevant. In future, the extent of introgression could be investigated using a wider suite of  
430 nuclear markers, such as single-nucleotide polymorphisms.

431

#### 432 4.2. Mainland biogeography

433 The *Panesthia* were found to have diverged from Melanesian ancestors in the late  
434 Miocene (ca. 7.62 Ma). By this point, paleobotanic and phylogeographic data suggest that  
435 rainforest had substantially retracted, with both mesic and sclerophyllous elements occurring  
436 across the eastern seaboard (Byrne et al., 2011; Martin, 2006; Rix and Harvey, 2012).  
437 Nonetheless, the ancestral *Panesthia* were inferred to be wet-forest obligates. A rainforest  
438 origin is concordant with the ecology of the genus in Southeast Asia (Roth, 1979b; Wang et  
439 al., 2014), although the precise relationships between Australian and Melanesian species are  
440 unclear because much of the latter's diversity remains undescribed. A wider body of evidence

441 also indicates that faunal exchange from Asia was dominated by rainforest species (e.g.,  
442 Braby et al., 2020; Rowe et al., 2011; Roycroft et al., 2022), suggesting that paleobotanic  
443 conditions were favorable to their dispersal.

444 The *Panesthia* now attain their greatest diversity in Queensland, comprising nine  
445 potential species. In sharp conflict with the hypothesis that rainforest patches were colonized  
446 by woodland-adapted ancestors (Beasley□Hall et al., 2021b; Roth, 1977), eight of these were  
447 found to have either retained the ancestral closed forest niche or only expanded into open  
448 forest (i.e., broadly remained within the mesic biome), with only a single transition to open  
449 woodland in the early-divergent species *P. parva*. The stem age of the species (ca. 4.02 Ma)  
450 coincides with a period of rapid woodland expansion, which may have driven this  
451 unidirectional xeric adaptation (e.g., Hugall et al., 2008; Rix et al., 2021). *Panesthia parva*  
452 displays a unique ecology among the genus, residing in dry, dead treetops and subsisting for  
453 months without moisture (J.A. Walker, pers. obs.). Potentially, the associated physiological  
454 and behavioral adaptations prohibit a reversion to inhabiting rainforest.

455 Our results suggest that most species arose through vicariance as mesic forests  
456 retracted. The two most speciose clades were found to occur primarily in the Northern and  
457 Central Queensland bioregions (Clades B+C; Figure 3). The boundary between these two  
458 regions corresponds to the Saint Lawrence Gap, an expanse of dry grassland that forms an  
459 arid barrier to dispersal in mesic organisms (Bryant and Krosch, 2016). While the timing of  
460 its formation is not resolved with high precision, a number of phylogeographic studies have  
461 detected divergences across the gap that date to the mid Pliocene (Baker et al., 2008; Burke et  
462 al., 2013; Chapple et al., 2011). This timeframe corresponds to the divergence between the  
463 two *Panesthia* clades (ca. 3.87 Ma) and suggests that they may have been isolated by the  
464 grasslands' formation. Ecological surveys undertaken by the authors have failed to detect  
465 *Panesthia* within the gap, indicating that it remains a barrier to this day.

466 Within the two clades, OTUs were found to typically occupy small habitat ranges,  
467 spanning one or few patches of rainforest or fringing open forest (i.e., *P. ancaudelliooides*, *P.*  
468 sp. Cape Upstart, *P.* sp. Brandy Creek, *P. cibrata* North, *P. matthewsi*; Figure 2). Micro-  
469 endemism is common in dispersal-limited invertebrates, which can persist long-term in small  
470 forest isolates (e.g., Harvey et al., 2017; Oberski et al., 2018). Based on our time-calibrated  
471 phylogeny, most speciation occurred during the Pliocene (ca. 2.5–5 Ma). During this period,  
472 intense glacial and interglacial cycles are thought to have caused substantial and rapid  
473 retractions in rainforest (Hill, 1994; White, 1986, 1994), producing the highly fragmented  
474 distribution seen today. In concordance, species-level structure dated to the Pliocene has been  
475 observed in many mesic lineages across the eastern seaboard (Baker et al., 2008; Heimburger  
476 et al., 2022; Lucky, 2011; Moreau et al., 2015; Mutton et al., 2019; Ponniah and Hughes,  
477 2004; Sota et al., 2005).

478 In contrast to the fine-scale endemism observed in northern and central Queensland,  
479 the southern reaches of the group's range are occupied by *P. cibrata* Central + South, which  
480 span larger, contiguous distributions from southern Queensland to Victoria. The boundary  
481 between the two corresponds to a region of dry sclerophyll, which presumably limits  
482 secondary contact (the Brisbane Valley Barrier; Bryant and Krosch, 2016). While present  
483 sampling did not cover the complete range of *P. cibrata* South, genetic relationships within  
484 the OTUs were not consistently arranged by geographic locality or habitat type, and close  
485 relationships were found between samples from distant rainforest and dry forest sites (e.g.,  
486 Mogo, Capertee Valley and Kempsey). This contrasts with the stricter geographic clustering  
487 and deeper structure seen in co-occurring rainforest invertebrates (Garrick et al., 2004;  
488 Garrick et al., 2008; Garrick et al., 2012; Symula et al., 2008) and suggests ongoing gene  
489 flow between wet and dry sclerophyll populations. Thus, our findings suggest that both

490 niche-conserved vicariance and more recent dispersal through drier forest have contributed to  
491 the contemporary distribution of the *Panesthia*.

492 Finally, secondary calibration with date estimates from Beasley-Hall et al. (2021b)  
493 yielded a substantially deeper evolutionary timescale. Under this scenario, the speciation of  
494 the *Panesthia* would have occurred against a backdrop of more gradual Miocene  
495 aridification, associated with the incipient fragmentation of east-coast rainforests (Byrne et  
496 al., 2011). A number of studies have estimated comparable (e.g., Lucky, 2011; Rix and  
497 Harvey, 2012; Tallowin et al., 2019) – or older (Gunter et al., 2019; Oberski et al., 2018) –  
498 species ages across the eastern seaboard, indicating that some or all of the biogeographic  
499 barriers between *Panesthia* clades may have formed during the Miocene. Thus, we cannot  
500 rule out this alternative explanation for the group's evolution.

501

502 *4.3. Colonization of the Lord Howe Island Group*

503 The Lord Howe Island cockroach *P. lata* is one of the most poorly understood  
504 members of the genus. Previous studies have only included one (Beasley-Hall et al., 2021b;  
505 Legendre et al., 2017; Legendre et al., 2015) or two (Lo et al., 2016) representatives of the  
506 species, leaving open questions regarding the timing, route and number of dispersals to the  
507 LHIG. By sampling across the full spatial extent of the LHIG, we robustly resolve *P. lata* as a  
508 monophyletic group and evidence the species reaching the islands in a single dispersal event.  
509 Our analyses also reveal appreciable population structure across the archipelago, which we  
510 discuss elsewhere in a focused population genetic investigation of the species (Adams et al.,  
511 in prep.).

512 The LHIG is highly remote, and the ancestors of *P. lata* presumably arrived by  
513 rafting. Range reconstructions based on the mitogenomic topology were unable to clearly  
514 estimate a biogeographic region of origin; however, the species was united with *P. cibrata*

515 South, which is found in New South Wales and far-southern Queensland. The LHIG occurs  
516 due east of Port Macquarie, New South Wales, thus a parsimonious explanation is that the  
517 islands were colonized from a nearby section of the mainland. However, we note that the  
518 phylogenies estimated from nuclear or concatenated mito-nuclear markers instead unite *P.*  
519 *lata* with species occurring further north in Queensland. In which case, propagules could  
520 potentially have been transported southwards by surface currents, following the establishment  
521 of the East Australian Current at least by the mid-Pliocene (Christensen et al., 2021;  
522 Przeslawski et al., 2011). Although biogeographic studies of LHIG terrestrial fauna are  
523 scarce, a sister relationship with Queensland species has been found in endemic *Armadillo*  
524 isopods (Lillemets and Wilson, 2002) and peloridiid moss bugs (Burckhardt, 2009). Similar  
525 patterns are also observed across a large range of marine taxa (e.g., Colgan and Woods, 2022;  
526 Veron and Done, 1979; Williams et al., 2011a).

527 *Panesthia lata* is notable for its tolerance of the uniquely exposed conditions on the  
528 small islets surrounding Lord Howe Island proper. Yet, even when accounting for its  
529 discordant placement between topologies, *P. lata* was consistently nested among rainforest or  
530 sclerophyllous lineages, and its ancestral habitat was inferred to be either closed or open  
531 forest. This suggests that the species initially established in rainforest, which is widespread  
532 on the main island, before subsequently expanding its environmental tolerance. Due to the  
533 non-monophyly of island populations within *P. lata* (Figure 1), it is challenging to discern  
534 precisely when and how the niche shift(s) occurred. Potentially, the species may have  
535 expanded its environmental tolerance early in its evolutionary history, and subsequently  
536 spread to the drier, more exposed islets. The label accompanying the samples from Ball's  
537 Pyramid, which diverged early in the species' history, indicates that they were collected from  
538 leaf litter (an unusually dry habitat for *Panesthia*). Alternatively, it is also plausible that niche  
539 expansions occurred multiple times in parallel, in association with the isolation of each islet

540 lineage. Further study is underway to investigate ecological differences among these  
541 populations and to refine hypotheses regarding their evolution.

542

543 *4.4. Wing morphology*

544 The *Panesthia* display a broad range of wing morphologies, spanning macropterous,  
545 brachypterous and micropterous forms. Even when accommodating the possibility of wing  
546 re-evolution (Forni et al., 2022), our reconstructions estimate that wing reduction has  
547 occurred 6–8 times independently, including at least twice within *P. cibrata* Central. Given  
548 the recency of diversification, possible explanations for the frequent wing reduction include  
549 *de novo* mutation, selection on standing polymorphism, or phenotypic plasticity. However,  
550 inconsistently with plasticity, wing morphs were strictly partitioned between allopatric  
551 populations, with no polymorphism at any single sampling locality. Long-term culture of  
552 *Panesthia* has also found wing morphology to be stable across generations (>10 years; H.A.  
553 Rose, J.A. Walker, pers. obs.). Therefore, it is likely that each instance of flight loss is  
554 independent, corroborating previous reports of frequent wing loss across the subfamily  
555 Panesthiinae (Bell et al., 2007b; Roth, 1977, 1979a, b, 1982).

556 The tendency towards wing reduction is presumably tied to the saproxylic niche. Due  
557 to the energetic maintenance costs of flight apparatus, wings are strongly selected against and  
558 frequently lost in confined habitats such as logs (Bell et al., 2007b; Roff, 1990). Likewise, the  
559 manual shedding of wings in macropterous lineages is ubiquitous, and presumably alleviates  
560 energetic costs through the histolysis of flight muscles (Roff, 1989; Tanaka, 1994). Hence, it  
561 is unclear how fitness varies between facultatively flightless (macropterous, wing-shed) and  
562 permanently flightless (wing-reduced) morphs, and whether any environmental pressures  
563 encourage permanent wing reduction.

564 One potential correlate that unites wing-reduced lineages is their occupation of small  
565 habitat patches. In addition to the island-endemic *P. lata*, all mainland flightless lineages  
566 have disjunct ranges spanning one or few mesic isolates. A long-standing hypothesis suggests  
567 that flight is selected against in insular habitats, to reduce dispersal into surrounding,  
568 unsuitable environments (reviewed by Waters et al., 2020). However, it is unknown how  
569 frequently, or how far, macropterous cockroaches fly prior to shedding. Measuring dispersal  
570 ability prior to wing-shedding would be needed to clarify the potentially deleterious nature of  
571 this trait in insular habitats. Likewise, habitat insularity may co-vary with other potentially  
572 relevant variables such as temperature, altitude or environmental stability (Roff, 1990, 1994),  
573 which were not considered in our habitat reconstructions. The presence of wing  
574 polymorphism in *P. cibrata* Central provides an exemplary model system in which to  
575 compare closely related, morphologically divergent populations. Fitness assays of different  
576 wing morphs of *P. cibrata* Central, complemented by more granular ecological and genomic  
577 analyses, could illuminate the underpinnings of this striking parallel evolution.

578

#### 579 4.5. Conclusions

580 This study provides new insights into the diversity of the *Panesthia*, revealing 11  
581 divergent genetic lineages. Niche reconstructions suggest that the ancestors of the group  
582 occupied closed mesic forest and subsequently speciated through both vicariance and  
583 transitions into drier forests as rainforests retracted during the Pliocene. The retraction of  
584 rainforest into insular refugia may have also driven parallel wing reduction by exerting  
585 selective pressure against flight, although further work is required to test this hypothesis. Our  
586 findings further reveal that *P. lata* most likely reached the LHIG in a single colonization  
587 event, and that the species expanded into a drier niche after establishment on the archipelago.

588 Overall, our integration of mainland and island taxa offers a holistic view of historical  
589 biogeography across two disparate geographic realms.

590

591 **Acknowledgements**

592 This project was supported by an Australia Pacific Science Foundation grant  
593 (APSF22029), and samples were collected under permits from NSW National Parks and  
594 Wildlife Services (SL102663) and the Lord Howe Island Board (05/22). The authors  
595 acknowledge the Sydney Informatics Hub and the use of the University of Sydney's high  
596 performance computing cluster, Artemis, for computational resources that contributed to  
597 results in the present paper. We are grateful to the Lord Howe Island Board for support and  
598 assistance with fieldwork, and to Chris Reid, Derek Smith, Jude Philip and Matthew Hahn for  
599 access to historical specimens. Finally, we thank Toby Kovacs for valuable comments on an  
600 earlier draft of the manuscript.

601

602 **Data availability**

603 The genomic sequences generated in this study are to be uploaded to GenBank prior  
604 to publication, and accession numbers will be provided in Supplementary Table S1.

605

606 **Conflict of interest**

607 The authors declare no conflicts of interest.

## References

- Allegrucci, G., Rampini, M., Chimenti, C., Alexiou, S., Di Russo, C., 2021. Dolichopoda cave crickets from Peloponnese (Orthoptera, Rhaphidophoridae): molecular and morphological investigations reveal four new species for Greece. *Eur. Zool. J.* 88, 505-524.
- Allegrucci, G., Trucchi, E., Sbordoni, V., 2011. Tempo and mode of species diversification in Dolichopoda cave crickets (Orthoptera, Rhaphidophoridae). *Mol. Phylogen. Evol.* 60, 108-121.
- Baker, C.H., Graham, G.C., Scott, K.D., Cameron, S.L., Yeates, D.K., Merritt, D.J., 2008. Distribution and phylogenetic relationships of Australian glow-worms *Arachnocampa* (Diptera, Keroplatidae). *Mol. Phylogen. Evol.* 48, 506-514.
- Bankevich, A., Nurk, S., Antipov, D., Gurevich, A.A., Dvorkin, M., Kulikov, A.S., Lesin, V.M., Nikolenko, S.I., Pham, S., Prjibelski, A.D., Pyshkin, A.V., Sirotnik, A.V., Vyahhi, N., Tesler, G., Alekseyev, M.A., Pevzner, P.A., 2012. SPAdes: a new genome assembly algorithm and its applications to single-cell sequencing. *J. Comput. Biol.* 19, 455-477.
- Barve, N., Barve, V., Jiménez-Valverde, A., Lira-Noriega, A., Maher, S.P., Peterson, A.T., Soberón, J., Villalobos, F., 2011. The crucial role of the accessible area in ecological niche modeling and species distribution modeling. *Ecol. Model.* 222, 1810-1819.
- Beasley-Hall, P.G., Rose, H.A., Bourguignon, T., Lo, N., 2021a. Molecular systematics and biogeography of an Australian soil-burrowing cockroach with polymorphic males, *Geoscapheus dilatatus* (Blattodea: Blaberidae). *Austral Entomol.* 60, 317-329.
- Beasley-Hall, P.G., Rose, H.A., Walker, J., Kinjo, Y., Bourguignon, T., Lo, N., 2021b. Digging deep: a revised phylogeny of Australian burrowing cockroaches (Blaberidae: Panesthiinae, Geoscapheinae) confirms extensive nonmonophyly and provides insights into biogeography and evolution of burrowing. *Syst. Entomol.* 46, 767-783.
- Beccaloni, G.W., 2014. Cockroach species file online. Version 5.0/5.0.

- Bell, K.L., Moritz, C., Moussalli, A., Yeates, D.K., 2007a. Comparative phylogeography and speciation of dung beetles from the Australian Wet Tropics rainforest. *Mol. Ecol.* 16, 4984-4998.
- Bell, W.J., Roth, L.M., Nalepa, C.A., 2007b. Cockroaches: ecology, behavior, and natural history. JHU Press.
- Bernt, M., Donath, A., Jühling, F., Externbrink, F., Florentz, C., Fritzsch, G., Pütz, J., Middendorf, M., Stadler, P.F., 2013. MITOS: Improved de novo metazoan mitochondrial genome annotation. *Mol. Phylogen. Evol.* 69, 313-319.
- Bourguignon, T., Lo, N., Cameron, S.L., Šobotník, J., Hayashi, Y., Shigenobu, S., Watanabe, D., Roisin, Y., Miura, T., Evans, T.A., 2014. The evolutionary history of termites as inferred from 66 mitochondrial genomes. *Mol. Biol. Evol.* 32, 406-421.
- Bourguignon, T., Tang, Q., Ho, S.Y., Juna, F., Wang, Z., Arab, D.A., Cameron, S.L., Walker, J., Rentz, D., Evans, T.A., 2018. Transoceanic dispersal and plate tectonics shaped global cockroach distributions: evidence from mitochondrial phylogenomics. *Mol. Biol. Evol.* 35, 970-983.
- Braby, M.F., Espeland, M., Müller, C.J., Eastwood, R., Lohman, D.J., Kawahara, A.Y., Maunsell, S.C., Pierce, N.E., 2020. Molecular phylogeny of the tribe Candalidini (Lepidoptera: Lycaenidae): systematics, diversification and evolutionary history. *Syst. Entomol.* 45, 703-722.
- Bryant, L.M., Krosch, M.N., 2016. Lines in the land: a review of evidence for eastern Australia's major biogeographical barriers to closed forest taxa. *Biol. J. Linn. Soc.* 119, 238-264.
- Burckhardt, D., 2009. Taxonomy and phylogeny of the Gondwanan moss bugs or Peloridiidae (Hemiptera, Coleorrhyncha). *Dtsch. Entomol. Z.* 56, 173-235.

- Burke, J.M., Ladiges, P.Y., Batty, E.L., Adams, P.B., Bayly, M.J., 2013. Divergent lineages in two species of *Dendrobium* orchids (*D. speciosum* and *D. tetragonum*) correspond to major geographical breaks in eastern Australia. *J. Biogeogr.* 40, 2071-2081.
- Byrne, M., Joseph, L., Yeates, D.K., Roberts, J.D., Edwards, D., 2018. Evolutionary History. In: Lambers, H. (Ed.), *On the Ecology of Australia's Arid Zone*. Springer International Publishing, Cham, 45-75.
- Byrne, M., Steane, D.A., Joseph, L., Yeates, D.K., Jordan, G.J., Crayn, D., Aplin, K., Cantrill, D.J., Cook, L.G., Crisp, M.D., 2011. Decline of a biome: evolution, contraction, fragmentation, extinction and invasion of the Australian mesic zone biota. *J. Biogeogr.* 38, 1635-1656.
- Cameron, S.L., Lo, N., Bourguignon, T., Svenson, G.J., Evans, T.A., 2012. A mitochondrial genome phylogeny of termites (Blattodea: Termitoidae): robust support for interfamilial relationships and molecular synapomorphies define major clades. *Mol. Phylogen. Evol.* 65, 163-173.
- Carstens, B.C., Pelletier, T.A., Reid, N.M., Satler, J.D., 2013. How to fail at species delimitation. *Mol. Ecol.* 22, 4369-4383.
- Chapple, D.G., Hoskin, C.J., Chapple, S.N.J., Thompson, M.B., 2011. Phylogeographic divergence in the widespread delicate skink (*Lampropholis delicata*) corresponds to dry habitat barriers in eastern Australia. *BMC Evol. Biol.* 11, 191.
- Che, Y., Deng, W., Li, W., Zhang, J., Kinjo, Y., Tokuda, G., Bourguignon, T., Lo, N., Wang, Z., 2022. Vicariance and dispersal events inferred from mitochondrial genomes and nuclear genes (18S, 28S) shaped global *Cryptocercus* distributions. *Mol. Phylogen. Evol.* 166, 107318.
- Christensen, B.A., De Vleeschouwer, D., Henderiks, J., Groeneveld, J., Auer, G., Drury, A.J., Karatsolis, B.T., Lyu, J., Betzler, C., Eberli, G.P., Kroon, D., 2021. Late Miocene Onset of

Tasman Leakage and Southern Hemisphere Supergyre Ushers in Near-Modern Circulation.

Geophys. Res. Lett. 48, e2021GL095036.

Colgan, D.J., Woods, C.L., 2022. Phylogeography and evolutionary dynamism of marine gastropods from the Lord Howe Island Group. Mar. Freshw. Res. 73, 884-899.

Djernæs, M., Varadinova, Z., Kotyl, M., Eulitz, U., Klass, K., 2020. Phylogeny and life history evolution of Blaberoidea (Blattodea). Arthropod Systematics & Phylogeny 78, 29-67.

Drummond, A.J., Ho, S.Y.W., Phillips, M.J., Rambaut, A., 2006. Relaxed phylogenetics and dating with confidence. PLoS Biol. 4, e88.

Ebach, M.C., 2017. Handbook of Australasian biogeography. CRC Press.

Ebach, M.C., Gill, A.C., Kwan, A., Ahyong, S.T., Murphy, D.J., Cassis, G., 2013. Towards an Australian bioregionalisation atlas: a provisional area taxonomy of Australia's biogeographical regions. Zootaxa 3619, 315–342-315–342.

Edgar, R.C., 2004. MUSCLE: multiple sequence alignment with high accuracy and high throughput. Nucleic Acids Res. 32, 1792-1797.

Forni, G., Martelossi, J., Valero, P., Hennemann, F.H., Conle, O., Luchetti, A., Mantovani, B., 2022. Macroevolutionary Analyses Provide New Evidence of Phasmid Wings Evolution as a Reversible Process. Syst. Biol. 71, 1471-1486.

Fourment, M., Holmes, E.C., 2016. Seqotron: a user-friendly sequence editor for Mac OS X. BMC Res. Notes 9, 1-4.

Garrick, R., Sands, C.J., Rowell, D.M., Tait, N., Greenslade, P., Sunnucks, P., 2004.

Phylogeography recapitulates topography: very fine□ scale local endemism of a saproxylic ‘giant’ springtail at Tallaganda in the Great Dividing Range of south-east Australia. Mol. Ecol. 13, 3329-3344.

- Garrick, R.C., Rowell, D.M., Simmons, C.S., Hillis, D.M., Sunnucks, P., 2008. Fine-scale phylogeographic congruence despite demographic incongruence in two low-mobility saproxylic springtails. *Evolution* 62, 1103-1118.
- Garrick, R.C., Rowell, D.M., Sunnucks, P., 2012. Phylogeography of saproxylic and forest floor invertebrates from Tallaganda, South-eastern Australia. *Insects* 3, 270-294.
- Gaunt, M.W., Miles, M.A., 2002. An insect molecular clock dates the origin of the insects and accords with palaeontological and biogeographic landmarks. *Mol. Biol. Evol.* 19, 748-761.
- Gunter, N.L., Monteith, G.B., Cameron, S.L., Weir, T.A., 2019. Evidence from Australian mesic zone dung beetles supports their Gondwanan origin and Mesozoic diversification of the Scarabaeinae. *Insect Syst. Evol.* 50, 162-188.
- Harvey, M.S., Rix, M.G., Harms, D., Giribet, G., Vink, C.J., Walter, D.E., 2017. The biogeography of Australasian arachnids. *Handbook of Australasian biogeography*. CRC Press, pp. 267-294.
- Heimburger, B., Schardt, L., Brandt, A., Scheu, S., Hartke, T.R., 2022. Rapid diversification of the Australian Amitermes group during late Cenozoic climate change. *Ecography* 2022, e05944.
- Hill, R.S., 1994. History of the Australian vegetation: Cretaceous to Recent. Cambridge University Press.
- Hipsley, C.A., Müller, J., 2014. Beyond fossil calibrations: realities of molecular clock practices in evolutionary biology. *Front. Genet.* 5, 138.
- Ho, S.Y., Lanfear, R., Bromham, L., Phillips, M.J., Soubrier, J., Rodrigo, A.G., Cooper, A., 2011. Time-dependent rates of molecular evolution. *Mol. Ecol.* 20, 3087-3101.
- Hoang, D.T., Chernomor, O., Von Haeseler, A., Minh, B.Q., Vinh, L.S., 2018. UFBoot2: improving the ultrafast bootstrap approximation. *Mol. Biol. Evol.* 35, 518-522.

- Hugall, A.F., Foster, R., Hutchinson, M., Lee, M.S.Y., 2008. Phylogeny of Australasian agamid lizards based on nuclear and mitochondrial genes: implications for morphological evolution and biogeography. *Biol. J. Linn. Soc.* 93, 343-358.
- Jin, M., Zwick, A., Ślipiński, A., de Keyzer, R., Pang, H., 2020. Museomics reveals extensive cryptic diversity of Australian prionine longhorn beetles with implications for their classification and conservation. *Syst. Entomol.* 45, 745-770.
- Kalyaanamoorthy, S., Minh, B.Q., Wong, T.K.F., von Haeseler, A., Jermiin, L.S., 2017. ModelFinder: fast model selection for accurate phylogenetic estimates. *Nat. Methods* 14, 587-589.
- Kinjo, Y., Saitoh, S., Tokuda, G., 2015. An Efficient Strategy Developed for Next-Generation Sequencing of Endosymbiont Genomes Performed Using Crude DNA Isolated from Host Tissues: A Case Study of *Blattabacterium cuenoti* Inhabiting the Fat Bodies of Cockroaches. *Microbes Environ.* 30, 208-220.
- Legendre, F., Grandcolas, P., Thouzé, F., 2017. Molecular phylogeny of Blaberidae (Dictyoptera, Blattodea) with implications for taxonomy and evolutionary studies. *Eur. J. Taxon.* 1-13.
- Legendre, F., Nel, A., Svenson, G.J., Robillard, T., Pellens, R., Grandcolas, P., 2015. Phylogeny of Dictyoptera: dating the origin of cockroaches, praying mantises and termites with molecular data and controlled fossil evidence. *PLoS One* 10, e0130127.
- Lillemets, B., Wilson, G.D., 2002. Armadillidae (Crustacea: Isopoda) from Lord Howe Island: new taxa and biogeography. *Rec. Aust. Mus.* 54, 71-98.
- Lo, N., Tong, K.J., Rose, H.A., Ho, S.Y., Beninati, T., Low, D.L., Matsumoto, T., Maekawa, K., 2016. Multiple evolutionary origins of Australian soil-burrowing cockroaches driven by climate change in the Neogene. *Proc. R. Soc. B.* 283, 20152869.

- Lucky, A., 2011. Molecular phylogeny and biogeography of the spider ants, genus *Leptomyrmex* Mayr (Hymenoptera: Formicidae). *Mol. Phylogen. Evol.* 59, 281-292.
- Maekawa, K., Lo, N., Rose, H.A., Matsumoto, T., 2003. The evolution of soil-burrowing cockroaches (Blattaria: Blaberidae) from wood-burrowing ancestors following an invasion of the latter from Asia into Australia. *Proc. R. Soc. B.* 270, 1301-1307.
- Martin, H., 2006. Cenozoic climatic change and the development of the arid vegetation in Australia. *J. Arid Environ.* 66, 533-563.
- Matzke, M.N.J., 2013. Package ‘BioGeoBEARS’.
- Matzke, N.J., 2022. Statistical comparison of DEC and DEC+ J is identical to comparison of two ClasSE submodels, and is therefore valid. *J. Biogeogr.* 49, 1805-1824.
- Minh, B.Q., Schmidt, H.A., Chernomor, O., Schrempf, D., Woodhams, M.D., von Haeseler, A., Lanfear, R., 2020. IQ-TREE 2: New Models and Efficient Methods for Phylogenetic Inference in the Genomic Era. *Mol. Biol. Evol.* 37, 1530-1534.
- Mitchell, K.J., Pratt, R.C., Watson, L.N., Gibb, G.C., Llamas, B., Kasper, M., Edson, J., Hopwood, B., Male, D., Armstrong, K.N., 2014. Molecular phylogeny, biogeography, and habitat preference evolution of marsupials. *Mol. Biol. Evol.* 31, 2322-2330.
- Moreau, C.S., Hugall, A.F., McDonald, K.R., Jamieson, B.G., Moritz, C., 2015. An ancient divide in a contiguous rainforest: Endemic earthworms in the Australian Wet Tropics. *PLoS One* 10, e0136943.
- Mutton, T.Y., Phillips, M.J., Fuller, S.J., Bryant, L.M., Baker, A.M., 2019. Systematics, biogeography and ancestral state of the Australian marsupial genus *Antechinus* (Dasyuromorphia: Dasyuridae). *Zool. J. Linn. Soc.* 186, 553-568.
- O'Neill, S., Rose, H., Rugg, D., 1987. Social behaviour and its relationship to field distribution in *Panesthia cribbrata* Saussure (Blattodea: Blaberidae). *Aust. J. Entomol.* 26, 313-321.

- Oberski, J.T., Sharma, P.P., Jay, K.R., Coblenz, M.J., Lemon, K.A., Johnson, J.E., Boyer, S.L., 2018. A dated molecular phylogeny of mite harvestmen (Arachnida: Opiliones: Cyphophthalmi) elucidates ancient diversification dynamics in the Australian Wet Tropics. *Mol. Phylogen. Evol.* 127, 813-822.
- Owens, H.L., Ribeiro, V., Saupe, E.E., Cobos, M.E., Hosner, P.A., Cooper, J.C., Samy, A.M., Barve, V., Barve, N., Muñoz-R, C.J., 2020. Acknowledging uncertainty in evolutionary reconstructions of ecological niches. *Ecol. Evol.* 10, 6967-6977.
- Papadopoulou, A., Anastasiou, I., Vogler, A.P., 2010. Revisiting the insect mitochondrial molecular clock: the mid-Aegean trench calibration. *Mol. Biol. Evol.* 27, 1659-1672.
- Ponniah, M., Hughes, J.M., 2004. The evolution of Queensland spiny mountain crayfish of the genus *Euastacus*. I. Testing vicariance and dispersal with interspecific mitochondrial DNA. *Evolution* 58, 1073-1085.
- Przeslawski, R., Williams, A., Nichol, S.L., Hughes, M.G., Anderson, T.J., Althaus, F., 2011. Biogeography of the Lord Howe rise region, Tasman sea. *Deep-Sea Res. II: Top. Stud. Oceanogr.* 58, 959-969.
- Puillandre, N., Brouillet, S., Achaz, G., 2021. ASAP: assemble species by automatic partitioning. *Mol. Ecol. Resour.* 21, 609-620.
- Rambaut, A., Drummond, A.J., Xie, D., Baele, G., Suchard, M.A., 2018. Posterior Summarization in Bayesian Phylogenetics Using Tracer 1.7. *Syst. Biol.* 67, 901-904.
- Ree, R.H., Sanmartín, I., 2018. Conceptual and statistical problems with the DEC+ J model of founder-event speciation and its comparison with DEC via model selection. *J. Biogeogr.* 45, 741-749.
- Revell, L.J., 2012. phytools: an R package for phylogenetic comparative biology (and other things). *Methods Ecol. Evol.* 3, 217-223.

- Ritchie, A.M., Lo, N., Ho, S.Y.W., 2016. The Impact of the Tree Prior on Molecular Dating of Data Sets Containing a Mixture of Inter- and Intraspecies Sampling. *Syst. Biol.* 66, 413-425.
- Rix, M.G., Harvey, M.S., 2012. Phylogeny and historical biogeography of ancient assassin spiders (Araneae: Archaeidae) in the Australian mesic zone: evidence for Miocene speciation within Tertiary refugia. *Mol. Phylogen. Evol.* 62, 375-396.
- Rix, M.G., Wilson, J.D., Huey, J.A., Hillyer, M.J., Gruber, K., Harvey, M.S., 2021. Diversification of the mygalomorph spider genus *Aname* (Araneae: Anamidae) across the Australian arid zone: Tracing the evolution and biogeography of a continent-wide radiation. *Mol. Phylogen. Evol.* 160, 107127.
- Roff, D.A., 1989. Exaptation and the evolution of dealation in insects. *J. Evol. Biol.* 2, 109-123.
- Roff, D.A., 1990. The evolution of flightlessness in insects. *Ecol. Monogr.* 60, 389-421.
- Roff, D.A., 1994. Habitat persistence and the evolution of wing dimorphism in insects. *Am. Nat.* 144, 772-798.
- Rose, H., 2003. Research Report on *Panesthia lata*, Blaberid cockroach 25-29 March 2003.
- Roth, L.M., 1977. A taxonomic revision of the Panesthiinae of the world. I. The Panesthiinae of Australia (Dictyoptera: Blattaria: Blaberidae). *Aust. J. Zool. Suppl. Ser.* 25, 1-112.
- Roth, L.M., 1979a. A taxonomic revision of the Panesthiinae of the world. II. The genera *Salgana* Stål *Microdina* Kirby and *Caeparia* Stål (Dictyoptera: Blattaria: Blaberidae). *Aust. J. Zool. Suppl. Ser.* 27, 1-201.
- Roth, L.M., 1979b. A Taxonomic revision of the Panesthiinae of the world. III. The genera *Panesthia* Serville and *Miopanesthia* Saussure (Dictyoptera: Blattaria: Blaberidae). *Aust. J. Zool. Suppl. Ser.* 27, 1-276.
- Roth, L.M., 1982. A taxonomic revision of the panesthiinae of the world. IV. The genus *Ancaudellia* Shaw, with additions to parts 1-3, and a general discussion of distribution and

- relationships of the components of the subfamily (Dictyopter: Blattaria: Blaberidae). *Aust. J. Zool. Suppl. Ser. 30*, 1-142.
- Rowe, K.C., Aplin, K.P., Baverstock, P.R., Moritz, C., 2011. Recent and Rapid Speciation with Limited Morphological Disparity in the Genus *Rattus*. *Syst. Biol.* 60, 188-203.
- Roycroft, E., Fabre, P.-H., MacDonald, A.J., Moritz, C., Moussalli, A., Rowe, K.C., 2022. New Guinea uplift opens ecological opportunity across a continent. *Curr. Biol.* 32, 4215-4224.e4213.
- Sota, T., Takami, Y., Monteith, G.B., Moore, B.P., 2005. Phylogeny and character evolution of endemic Australian carabid beetles of the genus *Pamborus* based on mitochondrial and nuclear gene sequences. *Mol. Phylogen. Evol.* 36, 391-404.
- Suchard, M.A., Lemey, P., Baele, G., Ayres, D.L., Drummond, A.J., Rambaut, A., 2018. Bayesian phylogenetic and phylodynamic data integration using BEAST 1.10. *Virus Evol.* 4, vey016.
- Symula, R., Keogh, J.S., Cannatella, D.C., 2008. Ancient phylogeographic divergence in southeastern Australia among populations of the widespread common froglet, *Crinia signifera*. *Mol. Phylogen. Evol.* 47, 569-580.
- Tallowin, O.J.S., Meiri, S., Donnellan, S.C., Richards, S.J., Austin, C.C., Oliver, P.M., 2019. The other side of the Sahulian coin: biogeography and evolution of Melanesian forest dragons (Agamidae). *Biol. J. Linn. Soc.* 129, 99-113.
- Tanaka, S., 1994. Evolution and physiological consequences of de-alation in crickets. *Res. Popul. Ecol.* 36, 137-143.
- Trueman, J., Pfeil, B., Kelchner, S., Yeates, D., 2004. Did stick insects really regain their wings? *Syst. Entomol.* 29, 138-139.
- Veron, J., Done, T.J., 1979. Corals and coral communities of Lord Howe Island. *Mar. Freshw. Res.* 30, 203-236.

- Wang, X., Wang, Z., Che, Y., 2014. A taxonomic study of the genus *Panesthia* (Blattodea, Blaberidae, Panesthiinae) from China with descriptions of one new species, one new subspecies and the male of *Panesthia antennata*. *ZooKeys* 53.
- Waters, J., Emerson, B.C., Arribas, P., McCulloch, G., 2020. Dispersal reduction: causes, genomic mechanisms, and evolutionary consequences. *Trends Ecol. Evol.* 35, 512-522.
- White, M.E., 1986. The greening of Gondwana. Reed, Frenchs Forest, NSW.
- White, M.E., 1994. After the greening: the browning of Australia. Kangaroo Press, Kenthurst, NSW.
- Williams, A., Althaus, F., Clark, M.R., Gowlett-Holmes, K., 2011a. Composition and distribution of deep-sea benthic invertebrate megafauna on the Lord Howe Rise and Norfolk Ridge, southwest Pacific Ocean. *Deep-Sea Res. II: Top. Stud. Oceanogr.* 58, 948-958.
- Williams, K., Ford, A., Rosauer, D., De Silva, N., Mittermeier, R., Bruce, C., Larsen, F., Margules, C., 2011b. Forests of East Australia: The 35th Biodiversity Hotspot. pp. 295-310.
- Xia, X., 2018. DAMBE7: New and improved tools for data analysis in molecular biology and evolution. *Mol. Biol. Evol.* 35, 1550-1552.
- Yang, Z., 2015. The BPP program for species tree estimation and species delimitation. *Curr. Zool.* 61, 854-865.
- Zhang, J., Kapli, P., Pavlidis, P., Stamatakis, A., 2013. A general species delimitation method with applications to phylogenetic placements. *Bioinformatics* 29, 2869-2876.
- Zink, R.M., Barrowclough, G.F., 2008. Mitochondrial DNA under siege in avian phylogeography. *Mol. Ecol.* 17, 2107-2121.
- Zwick, P., Zwick, A., 2023. Revision of the African *Neoperla* Needham, 1905 (Plecoptera: Perlidae: Perlinae) based on morphological and molecular data. *Zootaxa* 5316, 1-194.

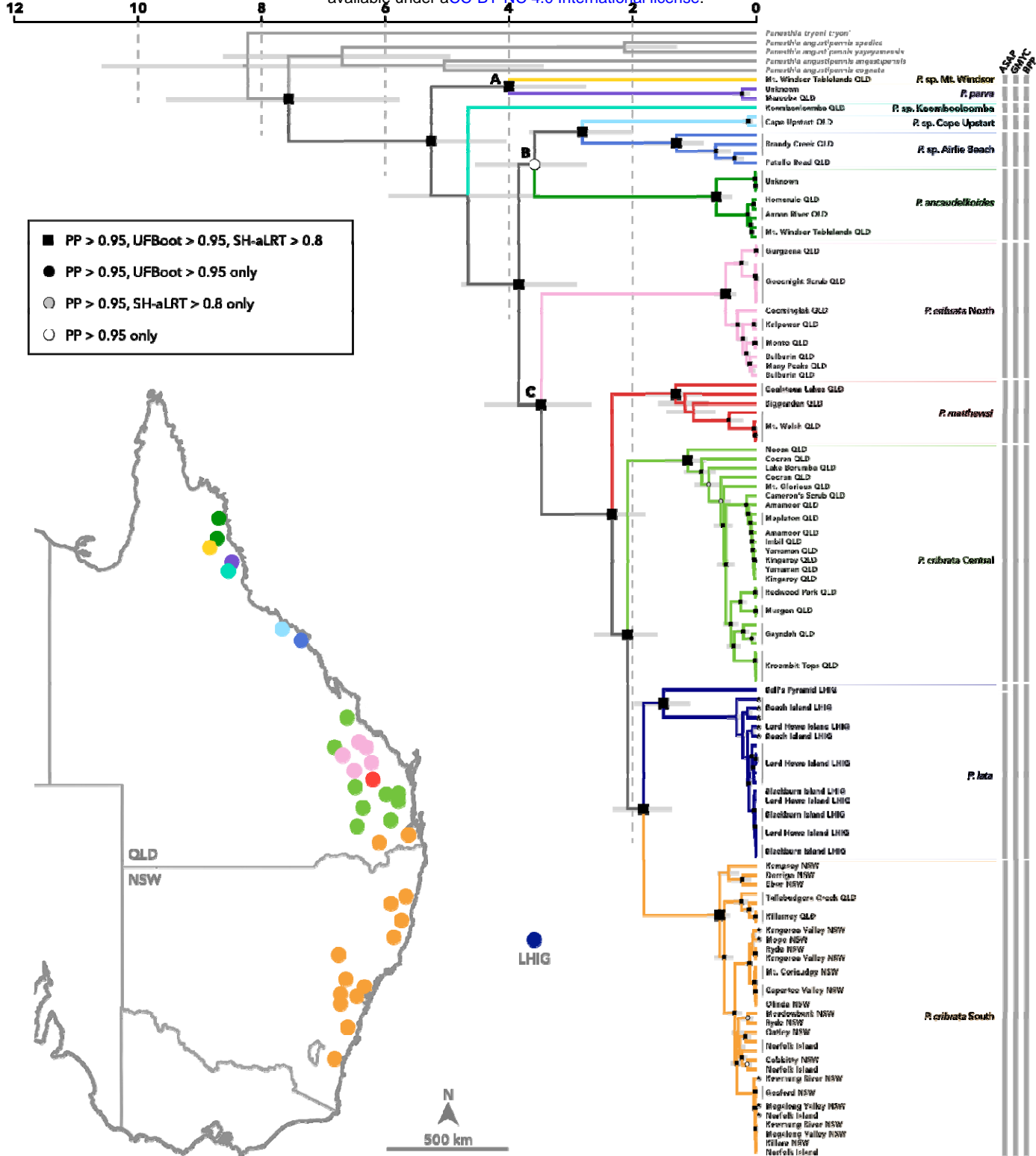


**Figure 1.** Dated phylogeny of the *Panesthia* inferred from complete mitochondrial genomes in BEAST and IQTREE. The evolutionary timescale was inferred using a previous estimate of the *COI* substitution rate (Allegrucci et al. 2011). PP: posterior probability, UFBoot: ultrafast bootstrap, SH-aLRT: SH-like approximate likelihood ratio test, QLD: Queensland,

NSW: New South Wales, LHIG: Lord Howe Island Group. Size of node labels varied for visual clarity. Letters A–C denote crown nodes of major clades. Stars denote tips with varying position between BEAST and IQTREE analyses. Results of species delimitation analyses are displayed to the right of tips. GMYC and ASAP results are based on mitochondrial genomes only, while BPP results are based on mitochondrial genomes and the nuclear ribosomal operon. Nomenclature and coloration of operational taxonomic units follows BPP results. **Inset:** distribution of sampling localities in eastern Australia.

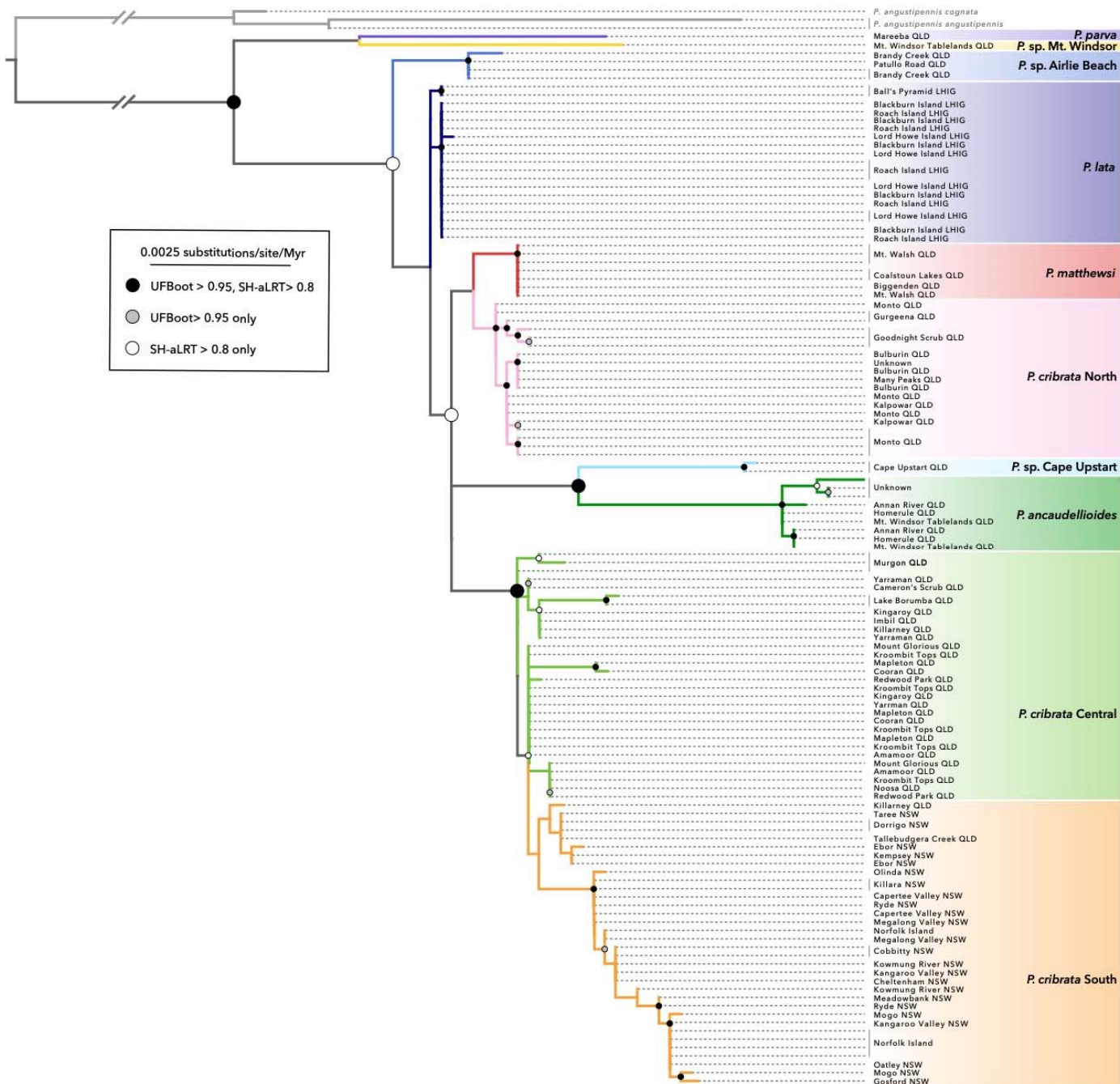


**Figure 2.** Maximum-likelihood phylogeny of the *Panesthia* inferred from the nuclear ribosomal operon in IQTREE. UFBoot: ultrafast bootstrap, SH-aLRT: SH-like approximate likelihood-ratio test. Sizes of node labels varied for visual clarity. Nomenclature and coloration of operational taxonomic units follows the mitogenomic (BPP) results.

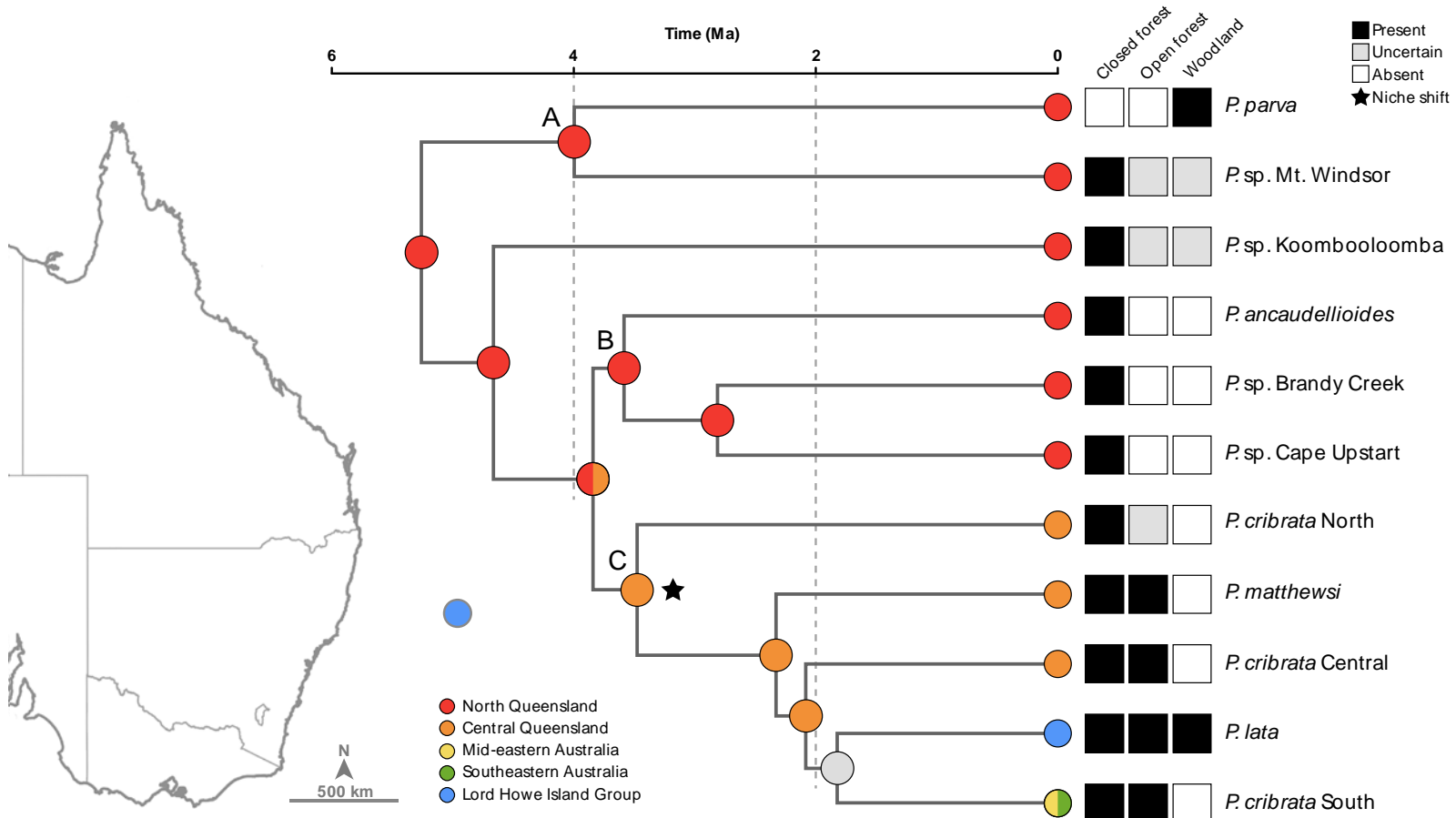


**Figure 3.** Ancestral geographic ranges and habitat niches of the *Panesthia*, reconstructed over the Bayesian chronogram inferred from whole mitogenomes in BEAST. Circles at nodes represent the most likely ancestral range, estimated using a dispersal-vicariance model in BioGeoBEARS. Multicolored circles denote a range spanning multiple bioregions, while a gray circle indicates an unresolved ancestral range. Tips are labeled with present-day distributions and habitat niches. The ancestral niche was inferred to be closed forest in *Nichevol* (not labeled), which was retained at all internal nodes until the point denoted by a star, where there was an inferred niche expansion into open forest.

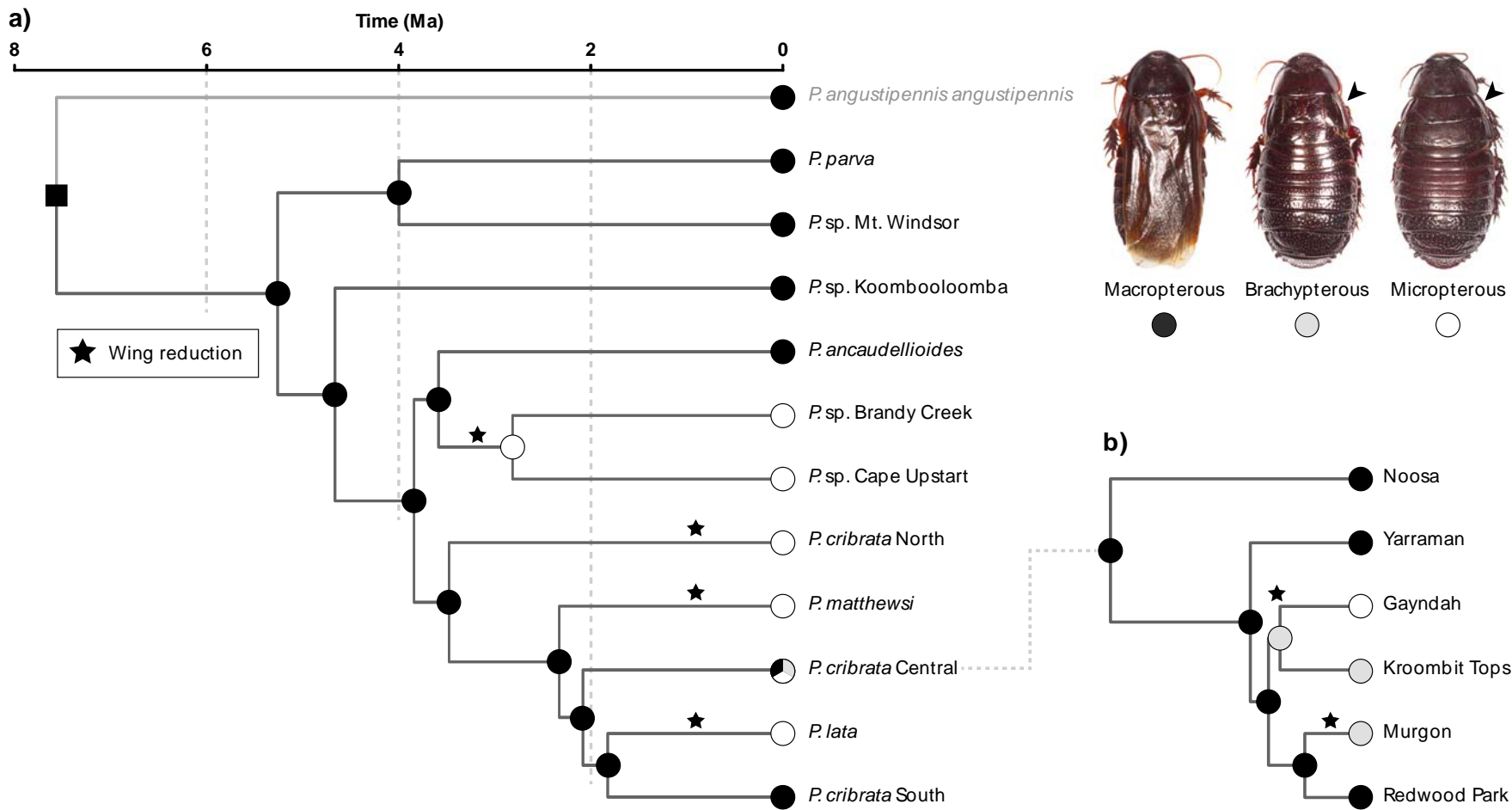


**Figure 4.** Evolution of wing morphology with wing re-evolution prohibited, reconstructed in *phytools* over the Bayesian chronogram inferred from complete mitogenomes in BEAST. **a)** Ancestral wing morphology of the 11 operational taxonomic units (OTUs). **b)** Ancestral wing morphology within the polymorphic OTU *Panesthia cibrata* Central, pruned to include a representative selection of sampling localities. Circles at nodes indicate the most probable ancestral state and the square at the root node the fixed ancestral state. States at all internal nodes were

estimated with probability  $> 50\%$ . Stars denote an inferred reduction of wings from a macropterous ancestor. **Inset:** representative habitus images of wing morphs. Arrows indicate reduced forewings. Photographs by Braxton Jones.